

Spin- $\frac{3}{2}$ models on the Cayley tree – optimum ground state approach

H. Niggemann J. Zittartz

Institut für Theoretische Physik, Zülpicher Str. 77, D-50937 Köln

Abstract

We present a class of *optimum ground states* for spin- $\frac{3}{2}$ models on the Cayley tree with coordination number 3. The interaction is restricted to nearest neighbours and contains 5 continuous parameters. For all values of these parameters the Hamiltonian has parity invariance, spin-flip invariance, and rotational symmetry in the xy -plane of spin space. The global ground states are constructed in terms of a 1-parametric *vertex state model*, which is a direct generalization of the well-known *matrix product ground state* approach. By using recursion relations and the transfer matrix technique we derive exact analytical expressions for local fluctuations and longitudinal and transversal two-point correlation functions.

1 Introduction

The Cayley tree belongs to the category of *pseudo-lattices* [1]. Unlike regular lattices, which are usually defined in terms of periodic structures, the Cayley tree is generated by the following *recursive* scheme:

1. A *Cayley branch* of order 1 is a single lattice site.
2. A *Cayley branch* of order n is defined as a lattice site with $K+1$ bonds, to which K Cayley branches of order $n-1$ are attached, i.e. the branch has 1 unconnected bond.
3. A *Cayley tree* of order n is given by a *central* lattice site with $K+1$ bonds, to which $K+1$ branches of order $n-1$ are attached.

K is called the *connectivity*, $K+1$ is the *coordination number* of the Cayley tree. Figure 1 shows a finite Cayley tree with coordination number 3. In the thermodynamic limit $n \rightarrow \infty$ the Cayley tree is also known as the *Bethe lattice*.

An important property of the Cayley tree is that there is exactly one path from a lattice site i to another lattice site j . The *distance* $|i-j|$ between i and j is simply the number of edges on this path. We can use the distance function to divide the Cayley tree into two disjoint sublattices. Denote the central site by i_0 . An arbitrary lattice site i belongs to the sublattice \mathcal{L}_A if $|i_0-i|$ is even, otherwise i belongs to the sublattice \mathcal{L}_B . It is easy to see that every site $i \in \mathcal{L}_A$

Work performed within the research program of the Sonderforschungsbereich 341, Köln-Aachen-Jülich

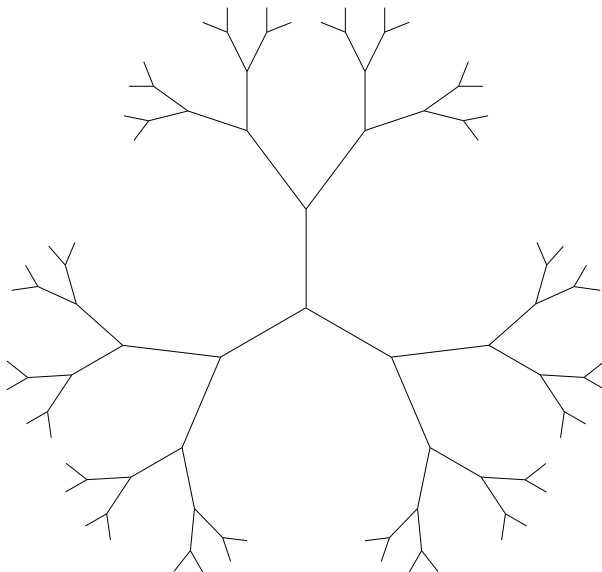


Figure 1: A finite Cayley tree with coordination number 3.

has only nearest neighbours in \mathcal{L}_B and vice versa, so $(\mathcal{L}_A, \mathcal{L}_B)$ is a *bipartite decomposition* of the Cayley tree. Note that it is valid for any connectivity K .

Due to the hierarchical structure of the lattice, the partition function of a classical statistical model on the Cayley tree can usually be calculated by using recursion relations, provided the local interaction has finite range and the number of states at each lattice site is also finite. This is a substantial step beyond models on the chain, as it allows to construct exactly solvable models *with arbitrary coordination number*. The most important drawback of the Cayley tree is that for large system sizes $\frac{1}{K}$ th of the lattice sites are boundary sites¹. As a consequence the physics is heavily influenced by boundary effects. There is no canonical way to impose periodic boundary conditions.

In this work we investigate the ground state problem of a class of quantum spin- $\frac{3}{2}$ models on the Cayley tree with connectivity $K = 2$. The paper is organized as follows. Section 2 contains the definition of the Hamiltonian and discusses its parameters and symmetries. The global ground state is constructed explicitly in section 3 in terms of a *vertex state model*. Vertex state models are graphical realizations of so-called *optimum ground states*, which simultaneously minimize all local interaction operators. Ground state properties, i.e. single-spin and two-point expectation values are presented in section 4. As shown in appendix A the calculation of ground state expectation values leads to a classical vertex model on the Cayley tree, which can be solved exactly. Finally we summarize our results in section 5.

¹For small system sizes the percentage of boundary sites is even larger.

2 Model definition

The model is defined on the Cayley tree with coordination number 3. A spin- $\frac{3}{2}$ is located at each lattice site. These spin variables are coupled by nearest neighbour interaction terms h_{ij} , which are all equal, they only act on different pairs of lattice sites. The global Hamiltonian H is the sum of all these local interactions, so the system is completely homogeneous.

The local interaction is the same as in our previous works on the hexagonal lattice [5] and the two-leg ladder [6]. Hence we shall be very brief here. For the construction of *optimum ground states* it is advantageous to write the interaction operator in terms of projectors onto its eigenstates

$$\begin{aligned}
 h_{ij} = & \lambda_3 (|v_3\rangle\langle v_3| + |v_{-3}\rangle\langle v_{-3}|) + \\
 & \lambda_2^{-\sigma} (|v_2^{-\sigma}\rangle\langle v_2^{-\sigma}| + |v_{-2}^{-\sigma}\rangle\langle v_{-2}^{-\sigma}|) + \\
 & \lambda_{12}^+ (|v_{12}^+\rangle\langle v_{12}^+| + |v_{-12}^+\rangle\langle v_{-12}^+|) + \\
 & \lambda_{02}^{-\sigma} |v_{02}^{-\sigma}\rangle\langle v_{02}^{-\sigma}|.
 \end{aligned} \tag{1}$$

If we use the following notation for the canonical basis states of a single spin- $\frac{3}{2}$,

$$\begin{aligned}
 S^z|3\rangle &= \frac{3}{2}|3\rangle & S^z|\bar{3}\rangle &= -\frac{3}{2}|\bar{3}\rangle \\
 S^z|1\rangle &= \frac{1}{2}|1\rangle & S^z|\bar{1}\rangle &= -\frac{1}{2}|\bar{1}\rangle,
 \end{aligned} \tag{2}$$

the eigenstates used in (1) are given by

$$\begin{aligned}
 |v_3\rangle &= |33\rangle \\
 |v_{-3}\rangle &= |\bar{3}\bar{3}\rangle \\
 |v_2^{-\sigma}\rangle &= |31\rangle - \sigma|13\rangle \\
 |v_{-2}^{-\sigma}\rangle &= |\bar{3}\bar{1}\rangle - \sigma|\bar{1}\bar{3}\rangle \\
 |v_{12}^+\rangle &= a|11\rangle - (|3\bar{1}\rangle + |\bar{1}3\rangle) \\
 |v_{-12}^+\rangle &= a|\bar{1}\bar{1}\rangle - (|\bar{3}1\rangle + |1\bar{3}\rangle) \\
 |v_{02}^{-\sigma}\rangle &= \sigma a^2 (|1\bar{1}\rangle - \sigma|\bar{1}1\rangle) - (|3\bar{3}\rangle - \sigma|\bar{3}3\rangle).
 \end{aligned} \tag{3}$$

The parameters $\lambda_3, \lambda_2^{-\sigma}, \lambda_{12}^+, \lambda_{02}^{-\sigma}$ are real and positive and the *superposition parameter* a is real. σ is a discrete parameter, which can only take the values ± 1 . Thus the total number of continuous parameters is 5, which includes a trivial scale, so there are 4 non-trivial interaction parameters.

For all values of the parameters h_{ij} (1) commutes with the pair magnetization operator $S_i^z + S_j^z$ and with the parity operator P_{ij} , which interchanges the spins at sites i and j . Therefore the local interaction (1) has rotational symmetry in the xy -plane of spin space and is parity invariant. In addition, corresponding eigenstates with magnetization m and $-m$ carry the same λ -coefficient, so h_{ij} is also invariant under a spin-flip $S^z \rightarrow -S^z$. In particular, no external magnetic field is applied.

As all λ -parameters are positive, (1) is a positive semi-definite operator, i.e. all its eigenvalues are non-negative. The two-spin states (3) are the excited local eigenstates of h_{ij} , the remaining 9 eigenstates are local ground states, i.e. the corresponding eigenvalue is zero. Since the Hamiltonian H is the sum of positive semi-definite operators, the global ground state energy E_0 is non-negative, too.

In the next section we shall show that E_0 is in fact zero and the corresponding global ground state will be constructed explicitly.

At the *isotropic point*, $a = -\sqrt{3}$ and $\sigma = -1$, the λ -parameters can be adjusted so that h_{ij} has the form

$$h_{ij} = \mathbf{S}_i \cdot \mathbf{S}_j + \frac{116}{243}(\mathbf{S}_i \cdot \mathbf{S}_j)^2 + \frac{16}{243}(\mathbf{S}_i \cdot \mathbf{S}_j)^3 + \frac{55}{108}. \quad (4)$$

Obviously, this operator has complete $SO(3)$ symmetry. It simply projects onto all states with $(\mathbf{S}_i + \mathbf{S}_j)^2 = 3(3+1)$. This case has already been investigated in [2]. Its ground state is known as the *valence bond solid* (VBS) ground state. As shown in [2], it has exponentially decaying correlation functions, no Néel order, and there is an energy gap between the ground state and the lowest excitations. This is consistent with our results presented in Section 4.

3 Construction of the global ground state

In this section we construct the exact ground state of the present model. It is an *optimum ground state* [3]–[6], i.e. it is not only the ground state of the global Hamiltonian H , but also of every local interaction operator h_{ij} . For spin chains such global states can be generated by using so-called *matrix product ground states* (MPG) [3, 4]. A generalization of the MPG concept to arbitrary lattices is given by *vertex state models* [4]–[6], which have been used to construct optimum ground states on the hexagonal lattice and on the two-leg ladder.

In order to construct the global ground state for the present model, we assign the following set of vertices to each site on the first sublattice of the Cayley tree:

$$\begin{array}{ll}
 \begin{array}{c} \leftarrow \bullet \nearrow \\ \leftarrow \bullet \nearrow \\ \leftarrow \bullet \nearrow \end{array} : \sigma a|3\rangle & \begin{array}{c} \leftarrow \bullet \nearrow \\ \leftarrow \bullet \nearrow \\ \leftarrow \bullet \nearrow \end{array} : \sigma a|\bar{3}\rangle \\
 \begin{array}{c} \leftarrow \bullet \nearrow \\ \leftarrow \bullet \nearrow \\ \leftarrow \bullet \nearrow \end{array} : |1\rangle & \begin{array}{c} \leftarrow \bullet \nearrow \\ \leftarrow \bullet \nearrow \\ \leftarrow \bullet \nearrow \end{array} : |\bar{1}\rangle \\
 \begin{array}{c} \leftarrow \bullet \nearrow \\ \leftarrow \bullet \nearrow \\ \leftarrow \bullet \nearrow \end{array} : |1\rangle & \begin{array}{c} \leftarrow \bullet \nearrow \\ \leftarrow \bullet \nearrow \\ \leftarrow \bullet \nearrow \end{array} : |\bar{1}\rangle \\
 \begin{array}{c} \leftarrow \bullet \nearrow \\ \leftarrow \bullet \nearrow \\ \leftarrow \bullet \nearrow \end{array} : |1\rangle & \begin{array}{c} \leftarrow \bullet \nearrow \\ \leftarrow \bullet \nearrow \\ \leftarrow \bullet \nearrow \end{array} : |\bar{1}\rangle .
 \end{array} \quad (5)$$

The corresponding vertices on the second sublattice are

$$\begin{array}{ll}
 \begin{array}{c} \text{---} \circlearrowleft \\ \text{---} \circlearrowleft \\ \text{---} \circlearrowleft \end{array} : a|3\rangle & \begin{array}{c} \text{---} \circlearrowright \\ \text{---} \circlearrowright \\ \text{---} \circlearrowright \end{array} : \sigma a|\bar{3}\rangle \\
 \begin{array}{c} \text{---} \circlearrowleft \\ \text{---} \circlearrowleft \\ \text{---} \circlearrowright \end{array} : |1\rangle & \begin{array}{c} \text{---} \circlearrowright \\ \text{---} \circlearrowright \\ \text{---} \circlearrowleft \end{array} : \sigma|\bar{1}\rangle \\
 \begin{array}{c} \text{---} \circlearrowright \\ \text{---} \circlearrowright \\ \text{---} \circlearrowleft \end{array} : |1\rangle & \begin{array}{c} \text{---} \circlearrowleft \\ \text{---} \circlearrowleft \\ \text{---} \circlearrowright \end{array} : \sigma|\bar{1}\rangle \\
 \begin{array}{c} \text{---} \circlearrowleft \\ \text{---} \circlearrowleft \\ \text{---} \circlearrowright \end{array} : |1\rangle & \begin{array}{c} \text{---} \circlearrowright \\ \text{---} \circlearrowright \\ \text{---} \circlearrowleft \end{array} : \sigma|\bar{1}\rangle .
 \end{array} \tag{6}$$

Unlike a *classical* vertex model, each vertex has a single-spin state $\alpha|m\rangle$ as its value (or ‘weight’), where

$$m = \frac{1}{2}(\# \text{ of outgoing arrows} - \# \text{ of incoming arrows}). \tag{7}$$

The parameters a and σ are the same as in (3). Both sets of vertices differ only with respect to the positions of the σ -coefficients. Note that (5) and (6) are the same as on the hexagonal lattice [5], only the global lattice topology is different.

The global ground state $|\Psi_0\rangle$ is generated by concatenating the vertices at all lattice sites. As in usual classical vertex models of statistical physics, the connecting bond between adjacent lattice sites is summed out. The generic product of vertex weights is replaced by the tensorial product in spin space:

$$\begin{array}{c}
 \begin{array}{c} \text{---} \bullet \text{---} \circlearrowleft \\ \text{---} \bullet \text{---} \circlearrowleft \\ \text{---} \bullet \text{---} \circlearrowleft \end{array} = \begin{array}{c} \begin{array}{c} \text{---} \bullet \text{---} \otimes \text{---} \circlearrowleft \\ \text{---} \bullet \text{---} \otimes \text{---} \circlearrowleft \\ \text{---} \bullet \text{---} \otimes \text{---} \circlearrowleft \end{array} \\
 + \\
 \begin{array}{c} \begin{array}{c} \text{---} \bullet \text{---} \otimes \text{---} \circlearrowright \\ \text{---} \bullet \text{---} \otimes \text{---} \circlearrowright \\ \text{---} \bullet \text{---} \otimes \text{---} \circlearrowright \end{array}
 \end{array} \tag{8}$$

It can be shown that the resulting global state is indeed an optimum ground state of H by collecting all two-spin states which are generated by all possible

concatenations of neighbouring vertices²:

$$\begin{aligned}
|31\rangle + \sigma|13\rangle & & |\overline{31}\rangle + \sigma|\overline{13}\rangle \\
|11\rangle + a|3\overline{1}\rangle & & |\overline{11}\rangle + a|\overline{31}\rangle \\
|11\rangle + a|\overline{13}\rangle & & |\overline{11}\rangle + a|1\overline{3}\rangle \\
|1\overline{1}\rangle + \sigma a^2|3\overline{3}\rangle & & |\overline{11}\rangle + \sigma a^2|\overline{33}\rangle \\
|1\overline{1}\rangle + \sigma|\overline{11}\rangle & &
\end{aligned} \tag{9}$$

These 9 two-spin states are orthogonal on all excited local states (3), so (9) are the local ground states of h_{ij} . Therefore it is clear that any projection of $|\Psi_0\rangle$ onto the space of two adjacent lattice sites is a linear combination of local ground states. This yields

$$h_{ij}|\Psi_0\rangle = 0 \tag{10}$$

for all nearest neighbours i and j and hence also

$$H|\Psi_0\rangle = 0. \tag{11}$$

Since zero is a lower bound of the global ground state energy, the constructed vertex state model is indeed an optimum ground state of the global Hamiltonian H .

In contrast to regular lattices there is no canonical way to impose periodic boundary conditions on the Cayley tree, so open boundary conditions are used. In this case, the vertices on the boundary sites ('leaves') emanate *external bonds* which are not summed out. Independent of the arrow configuration on these external bonds, the resulting vertex state model is always an optimum ground state of H . Thus the ground state degeneracy grows exponentially with system size.

4 Properties of the ground state

Each arrow configuration $\{b\}$ on the external bonds generates an optimum ground state $|\Psi_0^{\{b\}}\rangle$ of H . The calculation of ground state expectation values requires taking the average over all these configurations

$$\langle A \rangle_{\Psi_0} = \frac{1}{B} \sum_{\{b\}} \langle A \rangle_{\Psi_0^{\{b\}}}. \tag{12}$$

B denotes the total number of such configurations. By using the techniques developed in appendices A and B, ground state expectation values of arbitrary single-spin observables and two-spin correlation functions can be obtained exactly. As described in appendix A, the average over all boundary arrow configurations is performed automatically. Note that the formulae given below hold for *all* system sizes, on which the considered observables can be applied (cf. appendix B). In particular the results are valid in the thermodynamic limit. This pathological effect occurs only on the Cayley tree, optimum ground states on regular lattices exhibit a non-trivial finite-size behaviour.

²Common prefactors have been omitted.

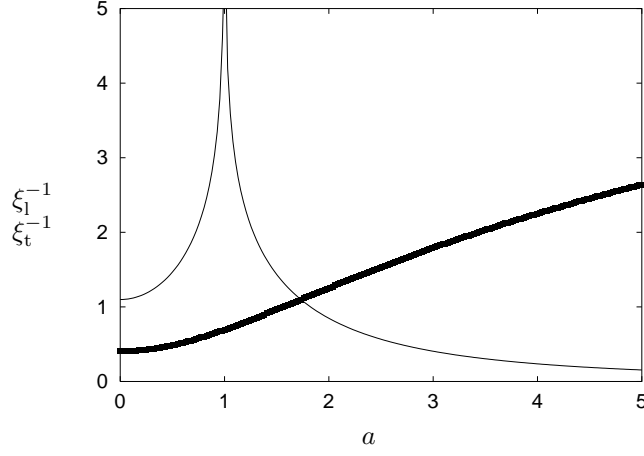


Figure 2: Inverse longitudinal (thin) and transversal (thick) correlation length as a function of the parameter a .

The first interesting expectation values are the components of the canonical spin operator

$$\langle S_i^x \rangle_{\Psi_0} = \langle S_i^y \rangle_{\Psi_0} = \langle S_i^z \rangle_{\Psi_0} = 0. \quad (13)$$

This is the expected result as the boundary conditions and the global ground states preserve the symmetries of the Hamiltonian, in particular spin-flip symmetry and rotational invariance in the xy -plane of spin space. (13) implies that the total magnetization is zero, so the global ground state is antiferromagnetic.

Although the local magnetization vanishes, its fluctuations are non-trivial

$$\langle (S_i^z)^2 \rangle_{\Psi_0} = \frac{9}{4} - \frac{6}{3+a^2}, \quad (14)$$

which increases monotonically from $\frac{1}{4}$ to $\frac{9}{4}$ as a function of a^2 , thus covering the full range of possible values. Because of rotational symmetry in the xy -plane of spin space we also obtain

$$\langle (S_i^x)^2 \rangle_{\Psi_0} = \langle (S_i^y)^2 \rangle_{\Psi_0} = \frac{1}{2} \left[\frac{3}{2} \left(\frac{3}{2} + 1 \right) - \langle (S_i^z)^2 \rangle_{\Psi_0} \right] = \frac{3}{4} + \frac{3}{3+a^2}. \quad (15)$$

In appendix B the transfer matrix technique has been employed to compute two-point correlation functions. The result for the longitudinal correlation function is

$$\langle S_i^z S_j^z \rangle_{\Psi_0} = - \left(\frac{1+3a^2}{6+2a^2} \right)^2 \cdot \left(\frac{1-a^2}{3+a^2} \right)^{|i-j|-1}, \quad (16)$$

where $|i-j|$ is the distance between lattice sites i and j . Note that the correlation decays exponentially as a function of the distance and its sign alternates if $a^2 > 1$. The corresponding longitudinal correlation length can be read off from equation (16). Its inverse is given by

$$\xi_l^{-1} = \ln \left| \frac{3+a^2}{1-a^2} \right|, \quad (17)$$

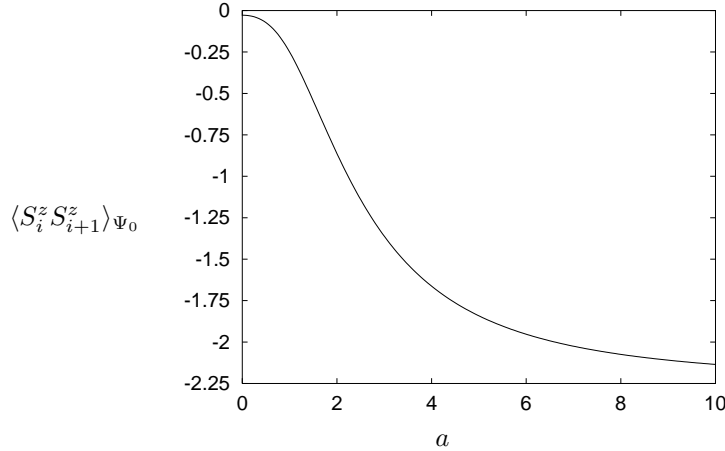


Figure 3: Longitudinal nearest-neighbour correlation as a function of the parameter a .

which is plotted as a function of the parameter a in figure 2. Note the divergence at $a = 1$. In this special case, longitudinal correlations between spins with a distance of 2 or larger are completely absent (cf. equation (16)).

As the longitudinal one, the transversal two-spin correlation function decays exponentially as a function of the distance:

$$\langle S_i^x S_j^x \rangle_{\Psi_0} = \left(\frac{2 + \sqrt{3} \sigma a}{3 + a^2} \right)^2 \cdot \left(\frac{2}{3 + a^2} \right)^{|i-j|-1}. \quad (18)$$

Thus the inverse transversal correlation length is

$$\xi_t^{-1} = \ln \frac{3 + a^2}{2}. \quad (19)$$

It is also plotted in figure 2, together with the longitudinal one. Both inverse correlation length, ξ_l^{-1} and ξ_t^{-1} , are non-zero for all finite values of a , hence the model is never critical.

In the special case $|i-j| = 1$ equation (16) yields the longitudinal nearest-neighbour correlation $\langle S_i^z S_{i+1}^z \rangle_{\Psi_0}$. Starting at $-\frac{1}{36}$ for $a = 0$ it decreases monotonically and approaches $-\frac{9}{4}$ asymptotically for large values of a , as shown in figure 3.

There are three noteworthy special points in the parameter space. The first one is $a^2 = 1$. In this case all non-vanishing vertices of the classical vertex model which corresponds to the inner product $\langle \Psi_0 | \Psi_0 \rangle$ (cf. appendix A) have the same weight, namely 1. This corresponds to infinitely high temperature in the language of classical vertex models, i.e. disorder is maximal. The vanishing of longitudinal correlations for $a^2 = 1$ (cf. figure 2) is consistent with this interpretation.

The next interesting special case is the isotropic point $a = -\sqrt{3}$, $\sigma = -1$ where we can adjust the λ -parameters so that the local interaction operator (1) has full $SO(3)$ symmetry. As mentioned in section 2, this model has already

been investigated in [2]. The reported inverse correlation length $\xi_{\text{iso}}^{-1} = \ln 3$ for open boundary conditions coincides with the results obtained from (17) and (19).

Finally we consider the limit $a^2 \rightarrow \infty$. As can be seen from (5) and (6) the global ground state is dominated by only four vertices in this limit, namely



on the first sublattice and



on the second one. The two ways, in which these vertices can be combined on the Cayley tree, represent the two different Néel states. All spins on the first sublattice are in the $|3\rangle$ state, the others are in the $|\bar{3}\rangle$ state, and vice versa. Therefore this special case is called the *Néel limit*. Note that the ground state degeneracy is higher than in the generic case. In addition to the degeneracy due to the open boundary conditions there is also a ‘bulk degeneracy’, as some of the local ground states (9) become simple tensor products of single-spin states.

5 Summary

We have investigated the ground state problem of a class of antiferromagnetic spin- $\frac{3}{2}$ models on the Cayley tree with coordination number 3. Apart from the lattice topology the Hamiltonian is the same as in our previous works on the hexagonal lattice [5] and the two-leg ladder [6]. It is defined in terms of the nearest neighbour interaction, which contains 5 continuous parameters and has parity invariance, spin-flip invariance, and rotational invariance in the xy -plane of spin space.

Due to the open boundary conditions the ground state degeneracy grows exponentially with system size. We have constructed the global ground states explicitly by using the *vertex state model* approach. These are so-called *optimum ground states*, i.e. they are not only ground states of the global Hamiltonian, but simultaneously minimize all local interaction operators. The vertex state model contains a continuous parameter a , which controls z -axis anisotropy, and a discrete parameter $\sigma = \pm 1$.

The calculation of ground state expectation values leads to a classical vertex model on the same lattice as the original quantum spin model. Due to the hierarchical structure of the Cayley tree this classical model can be solved exactly by using recursion relations and the transfer matrix technique. The result of our calculations is that the model has vanishing sublattice magnetization and exponentially decaying correlation functions. Exact formulae for the nearest neighbour correlation, the longitudinal and transversal correlation lengths, and for the fluctuations of the magnetization have been derived. For special values of a and σ the global ground state coincides with the so-called *valence bond solid* (VBS) ground state.

Appendix A: Calculation of single-spin expectation values

For the moment we consider only one of the many global ground states, namely the vertex state model with all boundary arrows pointing *out* of the leaf sites. Denote this ground state by $|\Psi_0^*\rangle$. Within this ground state, the expectation value of an observable A_i , which only acts on the spin at lattice site i , is defined as

$$\langle A_i \rangle_{\Psi_0^*} = \frac{\langle \Psi_0^* | A_i | \Psi_0^* \rangle}{\langle \Psi_0^* | \Psi_0^* \rangle}. \quad (\text{A.1})$$

The denominator can be interpreted as two identical vertex state models on top of each other, representing the bra- and the ket-vector, respectively. Since the vertices at each lattice site generate only local single-spin states, the inner product can be taken separately at each lattice site before the interior bonds are summed out. Hence $\langle \Psi_0^* | \Psi_0^* \rangle$ can be interpreted as the partition function of a *classical* vertex model with vertices defined as

$$\begin{array}{c} \mu_1 \\ \parallel \\ \bullet \\ \parallel \\ \mu_2 \\ \mu_3 \end{array} \begin{array}{c} v_2 \\ \parallel \\ \bullet \\ \parallel \\ v_3 \\ \mu_3 \end{array} = \left\langle \begin{array}{c} \mu_1 \\ \parallel \\ \bullet \\ \parallel \\ \mu_2 \\ \mu_3 \end{array} \right| \left| \begin{array}{c} v_2 \\ \parallel \\ \bullet \\ \parallel \\ v_3 \\ \mu_3 \end{array} \right\rangle. \quad (\text{A.2})$$

These vertices have the following properties:

- The vertex weights are real numbers, not single-spin states.
- There are two arrow variables on each bond, originating from the bra- and the ket-vector.
- The vertices are identical on both sublattices of the Cayley tree as $\sigma^2 = 1$.
- Only 20 of the 64 different vertices have a non-vanishing weight since the inner product between different S^z -eigenstates is zero.

The numerator of (A.1) corresponds to the same classical vertex model as the denominator, except for site i where the vertices are modified. At this special lattice site, the classical vertices are given by inserting the operator A_i between the bra- and the ket-vector on the r.h.s. of (A.2). The graphical representation of $\langle \Psi_0^* | A_i | \Psi_0^* \rangle$ is shown in figure 4. The affected site i is surrounded by three unmodified *branches* of the classical vertex model. In the following, these branches are denoted by $Z_n^{\leftarrow\leftarrow}$, $Z_n^{\rightarrow\rightarrow}$, $Z_n^{\leftarrow\rightarrow}$, and $Z_n^{\rightarrow\leftarrow}$, defined as

$$Z_n^{\mu\nu} = \begin{array}{c} \vdots \\ \bullet \\ \parallel \\ \mu \\ \parallel \\ \bullet \\ \parallel \\ \nu \\ \bullet \\ \parallel \\ \vdots \end{array} \quad (\text{A.3})$$

Here the lower index n denotes the order, i.e. the branch contains $2^n - 1$ lattice sites. Due to the hierarchical structure the values of (A.3) can be calculated by

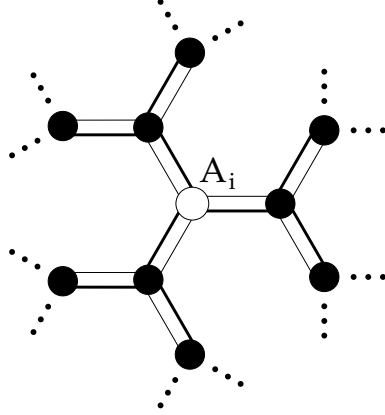


Figure 4: Graphical representation of single-spin expectation values.

using recursion relations. Each Z_{n+1} is given by concatenating two copies of Z_n to a single classical vertex and summing out the connecting bonds. This yields the recursion relations

$$\begin{aligned}
Z_{n+1}^{\leftarrow} &= \left(Z_n^{\leftarrow} + Z_n^{\rightarrow} \right)^2 + (a^2 - 1) \left(Z_n^{\rightarrow} \right)^2 + 2Z_n^{\rightarrow} Z_n^{\leftarrow} \\
Z_{n+1}^{\rightarrow} &= \left(Z_n^{\leftarrow} + Z_n^{\rightarrow} \right)^2 + (a^2 - 1) \left(Z_n^{\leftarrow} \right)^2 + 2Z_n^{\leftarrow} Z_n^{\rightarrow} \\
Z_{n+1}^{\rightarrow\leftarrow} &= \left(Z_n^{\leftarrow} + Z_n^{\rightarrow} \right) Z_n^{\rightarrow\leftarrow} \\
Z_{n+1}^{\leftarrow\rightarrow} &= \left(Z_n^{\leftarrow} + Z_n^{\rightarrow} \right) Z_n^{\leftarrow\rightarrow}.
\end{aligned} \tag{A.4}$$

In order to actually solve these coupled equations it is necessary to specify the initial values $Z_0^{\leftarrow}, Z_0^{\rightarrow}, Z_0^{\rightarrow\leftarrow}, Z_0^{\leftarrow\rightarrow}$ which are of course determined by the boundary conditions. For $|\Psi_0^*\rangle$, which is defined as having all boundary arrows pointing out of the leaf sites, the correct choice would be to set $Z_0^{\rightarrow} = 1$ and the other three initial values to zero³.

However, in order to calculate ground state expectation values, definition (12) requires the summation over all arrow configurations on the external bonds. It turns out that this summation can be carried out *automatically* by using the initial values

$$Z_0^{\leftarrow} = Z_0^{\rightarrow} = 1 \quad \text{and} \tag{A.5}$$

$$Z_0^{\leftarrow\rightarrow} = Z_0^{\rightarrow\leftarrow} = 0. \tag{A.6}$$

(A.5) ensures that configurations with incoming and outgoing arrows are weighted equally and (A.6) eliminates all ‘mixed’ terms, i.e. terms where bra- and ket-vector are different.

As a consequence of these initial values we obtain

$$Z_n^{\leftarrow} = Z_n^{\rightarrow} \quad \text{and} \tag{A.7}$$

$$Z_n^{\leftarrow\rightarrow} = Z_n^{\rightarrow\leftarrow} = 0 \tag{A.8}$$

³Multiplying the set of initial values with a common non-zero constant leaves all expectation values unchanged. So $Z_0^{\rightarrow} = 1$ is a convenient normalization.

for all $n \geq 0$. This is immediately clear from the recursion relations. Inserting (A.7),(A.8) into (A.4) yields

$$Z_{n+1}^{\leftarrow} = Z_{n+1}^{\rightarrow} = (3 + a^2) \left(Z_n^{\leftarrow} \right)^2, \quad (\text{A.9})$$

which has the solution

$$Z_n^{\leftarrow} = Z_n^{\rightarrow} = (3 + a^2)^{(2^n - 1)}. \quad (\text{A.10})$$

Note that the exponent $2^n - 1$ is simply the number of lattice sites of the branch. It is now straightforward to calculate the ground state expectation value of the local observable A_i as

$$\langle A_i \rangle_{\Psi_0} = \frac{Z(A_i)}{Z}. \quad (\text{A.11})$$

$Z(A_i)$ is given by attaching the solution (A.10) to all bonds of the classical vertex modified by the operator A_i (cf. figure 4). The denominator is simply

$$Z = Z(1) = 2(3 + a^2)^N, \quad (\text{A.12})$$

N being the total number of lattice sites. Due to the product structure of the solution (A.10) the results for all expectation values are *independent* of N . Additional powers of $3 + a^2$ drop out in the quotient (A.11). As shown in appendix B, a similar effect also occurs in the general case of k -point correlation functions. This means that there are *no finite size effects*. Note that although the classical vertex model has this simple product solution, the underlying vertex state model generates a highly non-trivial global ground state.

Equation (A.8) means that the classical vertex model contains *no unequal arrow pairs* on its bonds. The reason for this exact vanishing is that only classical vertices with zero or two unequal arrow pairs have a non-vanishing weight. Two of the three bonds of a leaf site are external bonds, which do not carry unequal arrow pairs (due to the open boundary conditions). So each leaf site provides the next hierarchy of vertices only with equal arrow pairs, and so on. Thus unequal arrow pairs can never enter the classical vertex model. This is in contrast to the hexagonal lattice [5], where unequal arrow pairs are in general present, albeit in a very low concentration for most values of the parameter a . This is a *dynamical* effect.

Appendix B: Calculation of two-spin expectation values

In this appendix we extend the technique developed in appendix A to two-point correlation functions $\langle A_i B_j \rangle_{\Psi_0}$. A_i and B_j are observables which only act on lattice sites i and j , respectively.

The Cayley tree is free of loops, so there is exactly one path from site i to site j . Figure 5 shows the topological structure of the corresponding classical vertex model. The branches $Z_n^{\mu\nu}$ are known from (A.8) and (A.10), so the remaining problem is the summation along the path from i to j . If $|i - j|$ denotes the

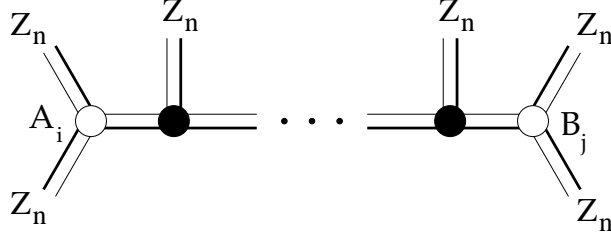


Figure 5: Graphical representation of two-spin correlation functions.

distance between these two lattice sites the path is given by the $(|i-j|-1)$ -fold product of the periodicity element⁴

$$\begin{array}{c}
 Z_n^{\mu\nu} \\
 | \\
 \mu \quad \nu \\
 \bullet \\
 \hline
 \mu_1 \quad \mu_2 \\
 \nu_1 \quad \nu_2
 \end{array}
 \quad (B.13)$$

The bonds $\mu_1\nu_1$ and $\mu_2\nu_2$ connect this element to the previous and to the next periodicity element on the path. The idea is to interpret (B.13) as a *transfer matrix* T [3, 4, 6] and to use its eigenbasis to calculate $T^{|i-j|-1}$.

Each bond carries two binary arrow variables, so T is a 4×4 -matrix. If the following mapping of arrow configurations to matrix indices is used

$$\begin{array}{ll}
 \leftarrow : 1 & \swarrow : 3 \\
 \rightarrow : 2 & \searrow : 4
 \end{array}
 \quad (B.14)$$

then the transfer matrix is given by

$$T = c_Z \begin{pmatrix} 2 & 1+a^2 & 0 & 0 \\ 1+a^2 & 2 & 0 & 0 \\ 0 & 0 & 2 & 0 \\ 0 & 0 & 0 & 2 \end{pmatrix}.
 \quad (B.15)$$

$c_Z = (3+a^2)^{(2^n-1)}$ is the prefactor due to the attached branch $Z_n^{\mu\nu}$. The eigenvalues χ_k and the corresponding normalized eigenvectors $|u_k\rangle$ of this real symmetric matrix are

$$\begin{array}{ll}
 \chi_1 = (3+a^2)c_Z & |u_1\rangle = (1, 1, 0, 0)/\sqrt{2} \\
 \chi_2 = (1-a^2)c_Z & |u_2\rangle = (1, -1, 0, 0)/\sqrt{2} \\
 \chi_3 = 2c_Z & |u_3\rangle = (0, 0, 1, 0) \\
 \chi_4 = 2c_Z & |u_4\rangle = (0, 0, 0, 1).
 \end{array}
 \quad (B.16)$$

This eigensystem can now be used to compute the desired powers of the transfer matrix as

$$T^{|i-j|-1} = \sum_k \chi_k^{|i-j|-1} |u_k\rangle\langle u_k|.
 \quad (B.17)$$

⁴Strictly speaking the order n of the branch $Z_n^{\mu\nu}$ can be different for each vertex along the path from site i to site j . However, for the same reason as in appendix A the order of these branches is completely irrelevant for the calculation of expectation values.

The final step is to assemble all components of the classical vertex model as shown in figure 5. To the left/right-hand side of (B.17) we attach the vertices modified by the observable A_i/B_j , respectively. Unmodified branches Z_n are attached to the remaining four bonds. In analogy to (A.11) the desired expectation value is given by

$$\langle A_i B_j \rangle_{\Psi_0} = \frac{Z(A_i, B_j)}{Z}. \quad (\text{B.18})$$

The numerator is the partition function of the modified vertex model calculated in this appendix and the denominator is the partition function of the *unmodified* vertex model $Z = 2(3 + a^2)^N$. As in the previous appendix, the average over all configurations of the boundary arrows is performed automatically.

Note that the order of the branch Z_n in (B.13) enters the calculation only via the factor c_Z which appears in all eigenvalues of T (B.16). However, c_Z drops out in the quotient (B.18), so the order of the branches attached to the path from site i to site j is irrelevant. The same holds for the four branches on the l.h.s. and on the r.h.s. of figure 5. Therefore the expectation value (B.18) only depends on the observables A_i and B_j and on their distance $|i - j|$. The size of the rest of the Cayley tree has no influence.

The technique developed in this appendix can be easily generalized to k -point correlation functions. If k is finite there is always a decomposition of the full lattice into a finite number of

- paths,
- modified vertices, and
- unmodified branches.

These objects can be dealt with separately. The resulting expectation values depend only on the observables themselves and the length of the paths between the vertices modified by these observables. The size of the unmodified branches is irrelevant. In this sense there are no finite size effects.

References

- [1] H. Moraal: *Classical, Discrete Spin Models*, Lecture Notes in Physics **214**, Springer-Verlag (1984)
- [2] I. Affleck, T. Kennedy, E.H. Lieb, H. Tasaki: *Comm. Math. Phys.* **115**, 477 (1988)
- [3] A. Klümper, A. Schadschneider, and J. Zittartz: *J. Phys.* **A24**, L955 (1991); *Z. Phys.* **B87**, 281 (1992); *Europhys. Lett.* **24**, 293 (1993)
- [4] H. Niggemann and J. Zittartz: *Z. Phys.* **B101**, 289 (1996)
- [5] H. Niggemann, A. Klümper, and J. Zittartz: *Z. Phys.* **B104**, 103 (1997)
- [6] H. Niggemann and J. Zittartz: preprint cond-mat/9808342